Journal of Asian Ceramic Societies 3 (2015) 292–300

HOSTED BY

Contents lists available at ScienceDirect

Journal of Asian Ceramic Societies

journal homepage: www.elsevier.com/locate/jascer

Characterization and optimization of electrospun TiO_2/PVP nanofibers using Taguchi design of experiment method

H. Albetran[a,b], Y. Dong[c], I.M. Low[a,*]

[a] Department of Imaging and Applied Physics, Curtin University, Perth, WA 6845, Australia
[b] Department of Basic Sciences, College of Education, University of Dammam, Dammam 31451, Saudi Arabia
[c] Department of Mechanical Engineering, Curtin University, Perth, WA 6845, Australia

ARTICLE INFO

Article history:
Received 3 March 2015
Received in revised form 1 May 2015
Accepted 5 May 2015
Available online 23 May 2015

Keywords:
Taguchi method
TiO_2/PVP nanocomposites
Electrospun nanofibers

ABSTRACT

TiO_2 nanofibers were prepared within polyvinylpyrrolidone (PVP) polymer using a combination of sol–gel and electrospinning techniques. Based on a Taguchi design of experiment (DoE) method, the effects of sol–gel and electrospinning on the TiO_2/PVP nanofibers' diameter, including titanium isopropoxide (TiP) concentration, flow rate, needle tip-to-collector distance, and applied voltage were evaluated. The analysis of DoE experiments for nanofiber diameters demonstrated that TiP concentration was the most significant factor. An optimum combination to obtain smallest diameters was also determined with a minimum variation for electrospun TiO_2/PVP nanofibers. The optimum combination was determined to be a 60% TiP concentration, at a flow rate of 1 ml/h, with the needle tip-to-collector distance at 11 cm (position *a*), and the applied voltage of 18 kV. This combination was further validated by conducting a confirmation experiment that used two different needles to study the effect of needle size. The average nanofiber diameter was approximately the same for both needle sizes in good accordance with the optimum condition estimated by the Taguchi DoE method.

1. Introduction

The electrospinning technique has attracted considerable attention as a relatively new, cheap and simple synthesis method for one-dimensional nanostructures [1–4]. The unique nanofibers prepared by electrospinning generally exhibit high surface area-to-volume ratios, high porosity, nanosized effects, and excellent mechanical strength [5]. They have been suggested for many applications, such as membrane separation, drug delivery, protective clothing, wound dressings, filtration, tissue engineering, and electronics [6–9].

Titanium dioxide (TiO_2), also known as titania, has emerged as a promising photocatalyst in the current market. It has the advantages of being photocatalytically stable, reasonably inexpensive, and relatively easy to produce and use. It is a human and environmentally friendly photocatalyst used to treat polluted air and water, and to split water to generate hydrogen [10]. A high surface area-to-volume ratio (SA/vol) of electrospun nanofibers can significantly improve the photocatalytic performance of TiO_2 because of small fiber size, and the high SA/vol provides further means for quick charge transfer to the dynamics of hole–electron (e^-/h^+) recombination on a large specific surface area of TiO_2 nanofibers [6,11].

TiO_2 nanofibers can be synthesized by combining electrospinning with a TiO_2 sol–gel technique [2,3,11–14]. The components of the electrospun experiment to synthesize TiO_2 nanofibers comprise a syringe pump, a syringe with a conductive needle, a high voltage supply, a conductive collector, copper wires, and a sol–gel of polymer (binder), and a TiO_2 precursor [4]. In general, electrospun nanofiber diameters depend primarily on three processing parameter sets [15] mentioned below.

The first set of adjusted parameters involved in the sol–gel solution include electrical conductivity, viscosity, surface tension, polymer concentration, and molecular weight. They are related to one another, and these relationships have important influences on electrospun nanofiber diameters [16]. The viscosity of the TiO_2 solution depends on the molecular weight and concentration of the material solution, such as polymer, solvent, and TiO_2 sources. The polymer concentration is one of the most significant factors in controlling beads and fiber diameters [16–18]. The TiO_2 fiber diameter

* Corresponding author. Tel.: +61 8 9266 7544; fax: +61 8 9266 2377.
E-mail address: j.low@curtin.edu.au (I.M. Low).
Peer review under responsibility of The Ceramic Society of Japan and the Korean Ceramic Society.

http://dx.doi.org/10.1016/j.jascer.2015.05.001

increases with a higher TiO_2 concentration in a precursor solution [12,19].

Electrospinning conditions are the second set of parameters, which consist of applied voltage, flow rate, needle size, and needle tip-to-collector distance [16]. Optimally applied voltage is a significant factor to affect fiber diameters [17,19–21]. High applied voltage (i.e., strong electrical repulsive forces) reduces the nanofiber diameter, resulting in highly stretched and elongated fibers [20]. Flow rate plays one of the most important roles in determining the fiber diameter and bead formation, because it determines the amount of sol–gel solution available to be stretched into nanofibers [16,19,20]. During the electrospinning process, the shape and size of the needle tip affect the formation of Taylor cone and nanofiber oscillation [22]. Ksapabutr et al. [22] claimed that a sawtooth needle shape allowed for Taylor cones of greater length than standard and flat counterparts. A needle tip-to-collector distance with the sufficient field gradient produces fibers with less bead defects, but the more considerable distance increases the nanofiber diameter owing to subsequent decreases in the electric field gradient [17]. Applied high voltage setting, a large needle tip-to-collector distance, a comparatively low concentration of polymer solutions and a low flow rate reduce the variation in product quality of electrospun fiber mats with a minimum number of experiments [17]. It is clear that the relationship between electrospun variables and associated fibrous structures is still not well understood to achieve ultrafine bead-free nanofibers with good dimensional stability.

Aspects of the atmospheric environment, such as humidity, pressure, and temperature, belong to the last set of parameters. The average nanofiber diameter decreases with increasing atmospheric temperature and decreasing atmospheric humidity [23].

Electrospun TiO_2/PVP nanofibers were synthesized using different titanium oxide precursors with a constant flow rate, needle tip-to-collector distance, and applied voltage in most electrospun experiments [2,8,28–31]. The fibers have a smooth and uniform surface with a random orientation, and the average fiber diameters range from 132 to 2280 nm [24–27]. Kumar and co-worker used a different applied voltage and flow rate with a constant needle-to-collector distance. At ~10 cm, the average diameter of the as-spun TiO_2/PVP nanofiber was 450 nm at 10 kV and 1 ml/h, 262 nm at 20 kV and 1 ml/h, and 145 nm at 20 kV and 0.5 ml/h [20].

The Taguchi method for robust experimental design is a useful engineering approach to select the optimal levels of processing parameters with the minimal sensitivity to different causes of variations. Furthermore, such a method can also elucidate the effects of a large and complex number of factors on an individual and interactive basis. In general, two essential tools are required, namely an orthogonal array (OA) to simultaneously accommodate several experimental design factors, and signal to noise ratio (S/N) to measure the most robust set of operating conditions from variations within the results [17,28–31].

In this study, TiO_2 nanofibers were fabricated with PVP polymer as precursor using both sol–gel and electrospinning techniques. An optimum combination of parameters obtained from TiP concentration, flow rate, needle tip-collector distance, and applied voltage in response to minimizing diameter size and its variation for TiO_2/PVP nanofibers was determined by means of the Taguchi DoE method. Such an optimum condition was further implemented to explore the effect of needle size on fiber diameters accordingly.

2. Experimental procedure

2.1. Materials

Titanium isopropoxide (TiP) (M_W = 284.22 g/mol, 97% purity), polyvinylpyrrolidone (PVP) (M_W = 1,300,000 g/mol, 100% purity),

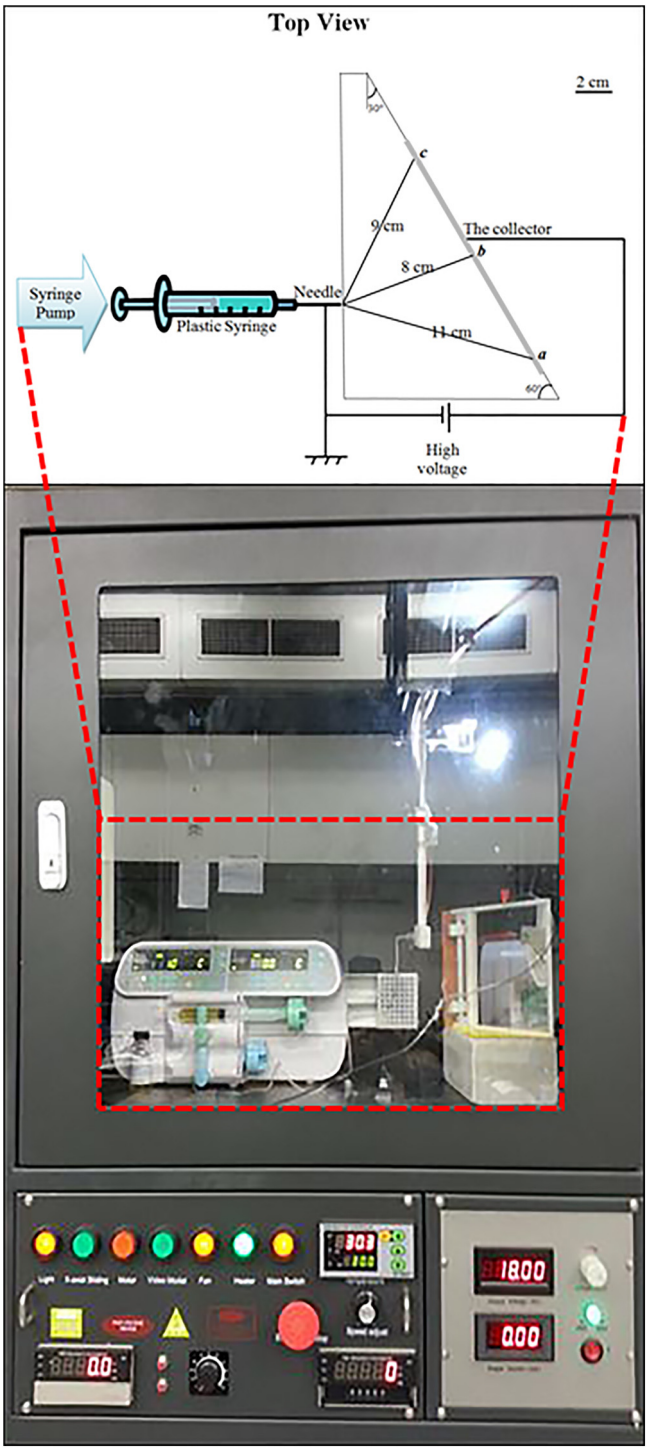

Fig. 1. Schematic diagram of electrospinning process with a slope collector.

acetic acid (M_W = 60.05 g/mol, 99.7% purity) and ethanol (M_W = 46.07 g/mol, 99.5% purity) were all purchased from Sigma–Aldrich, Inc., NSW, Australia.

2.2. Preparation of TiO_2/PVP sol–gel

TiO_2/PVP solutions were prepared by mixing 40 wt%, 50 wt% or 60 wt% TiP with a constant mixed solvent, which comprised 2.098 g acetic acid and 4.734 g ethanol (1:3 volume ratio) with 2.05 g PVP polymer inside a glass bottle. The solutions were subsequently subjected to magnetic stirring for 120 min at 80 °C. The viscosity of

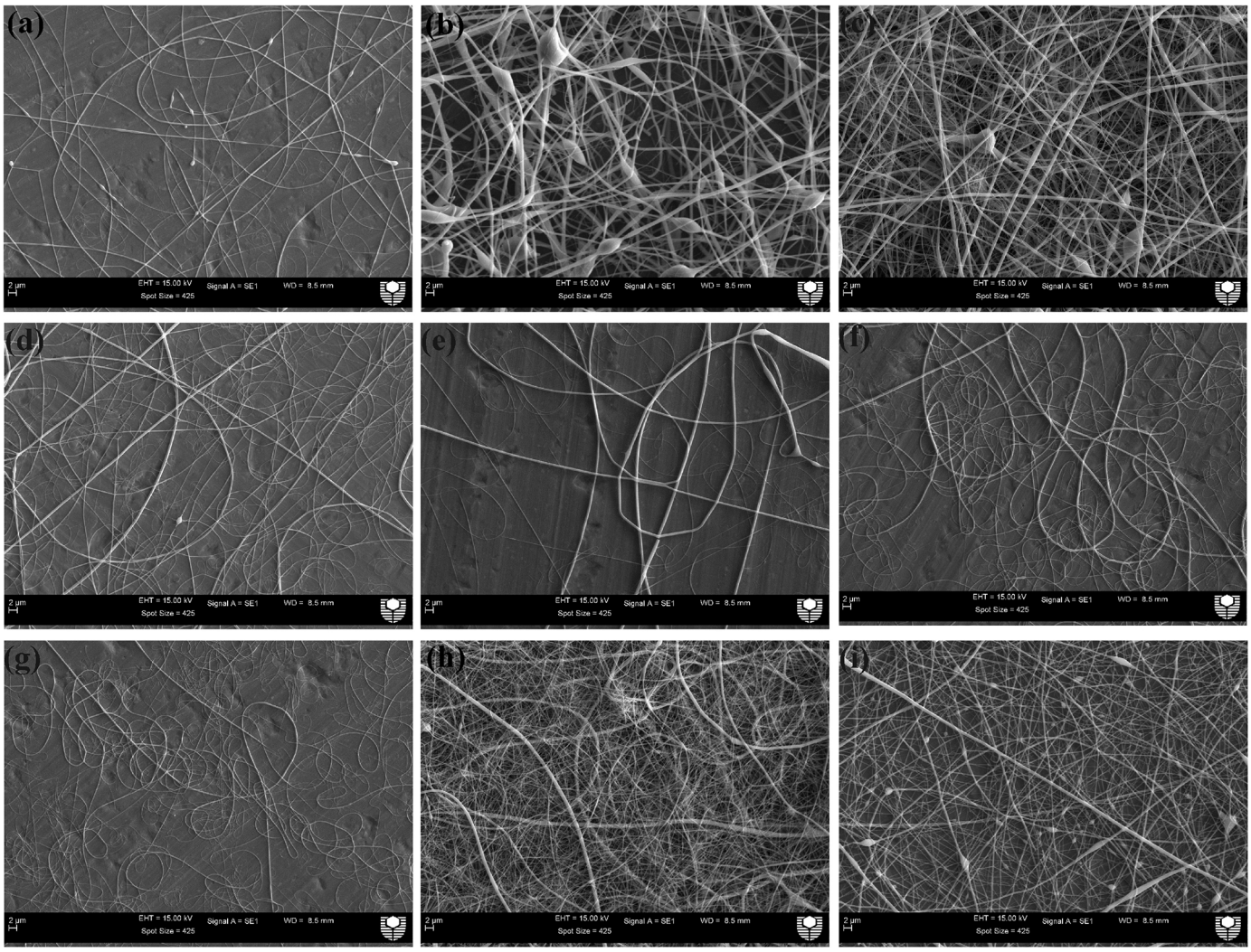

Fig. 2. SEM micrographs of electrospun TiO_2/PVP nanofibers used in DoE study: (a) T1, (b) T2, (c) T3, (d) T4, (e) T5, (f) T6, (g) T7, (h) T8, and (i) T9. All scale bars represent 2 μm.

the TiO_2/PVP solution depends on the concentration and molecular weight of PVP polymer, the solvent, and TiO_2 sources [3,12]. As the solvent and PVP were constant, the viscosities of the solutions were solely controlled by the TiP concentration (wt%). Increasing the TiP concentration (284.22 g/mol) reduces the concentration of PVP (1,300,000 g/mol), which further reduces the solution viscosity.

2.3. Electrospinning experiments

A commercial Nabond® electrospinning unit (standard type) was purchased from Nabond Technologies Co., Ltd., Shenzhen, China to fabricate electrospun fiber mats. The homogeneous solution was loaded into a 10 ml plastic syringe that was attached to a stainless steel needle with the inner diameter of approximately 0.514 mm. The needle tip-to-collector distance was varied due to a slope aluminum collector (see Fig. 1). Thus, the needle tip-to-collector distances were in range of ~11 cm for position *a*, ~8 cm for position *b*, and ~9 cm for position *c*. A syringe pump was used to control the solution flow rate at 0.5, 1, or 2 ml/h during the electrospinning process. The voltage setting was controlled by a high voltage power supply to maintain 14, 18, or 25 kV between the needle and the slope collector. The slope collector was covered

Table 1
Four factors and three levels selected in the DoE study for electrospun TiO_2/PVP nanofibers.

	Factor description	Level		
		1	2	3
A	TiP concentration (wt%)	40	50	60
B	Flow rate (ml/h)	0.5	1	2
C	Needle tip-to-collector distance (cm)	~11	~8	~9
D	Applied voltage (kV)	14	18	25

Table 2
Taguchi orthogonal array with nine trials (L_9).

Trial	Factor			
	A: TiP concentration (wt%)	B: flow rate (ml/h)	C: needle tip-to-collector distance (cm)	D: applied voltage (kV)
T1	40	0.5	a	14
T2	40	1	b	18
T3	40	2	c	25
T4	50	0.5	b	25
T5	50	1	c	14
T6	50	2	a	18
T7	60	0.5	c	18
T8	60	1	a	25
T9	60	2	b	14

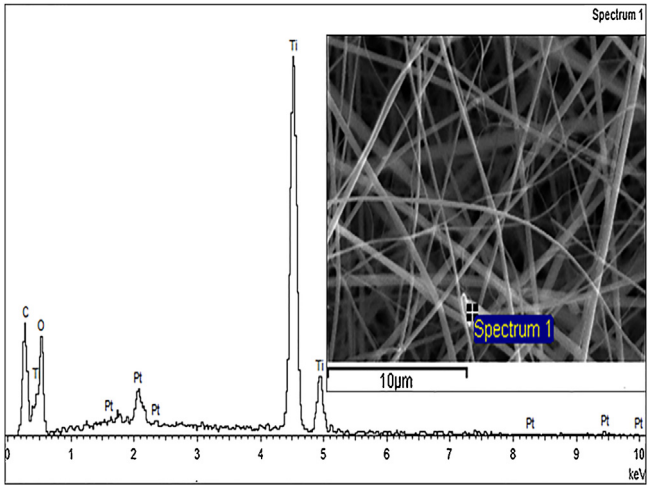

Fig. 3. EDS spectra of electrospun TiO_2/PVP nanofibers.

with an aluminum foil, and the needle tip-to-collector distance was adjusted accordingly. The electrospinning experiments were performed in a sealed environmental chamber at a constant temperature of 30 °C maintained by a lamp heater.

2.4. Taguchi DoE

Four factors of sol–gel and electrospinning parameters have been selected for this experiment, which are given by TiP concentration, flow rate, collector distance, and applied voltage at three different levels (Table 1). The full factorial experiment of 81 (3^4) trials can be completed in just 27 runs due to the slope collector, but that entails a large number of tests, which are significant in both experimental cost and time. As a result, Taguchi DoE layouts are more applicable when compared to a traditional full-factorial counterpart. This is because it reduced the number of tests to a practical level, thus significantly saving the experimental time and associated costs as opposed to the conduct of four factors individually. The L_9 DoE orthogonal array was selected with the assumption of no factorial interactions, resulting in nine trials as illustrated in Table 2.

2.5. Analysis of variance (ANOVA)

As earlier mentioned, the Taguchi DoE method replaces the full factorial experiments with only a simple orthogonal array of nine trials. To determine the significant factors, and optimum combination of factors, an analysis of variance (ANOVA) was utilized in order to offer a measure of confidence by determining and analyzing the

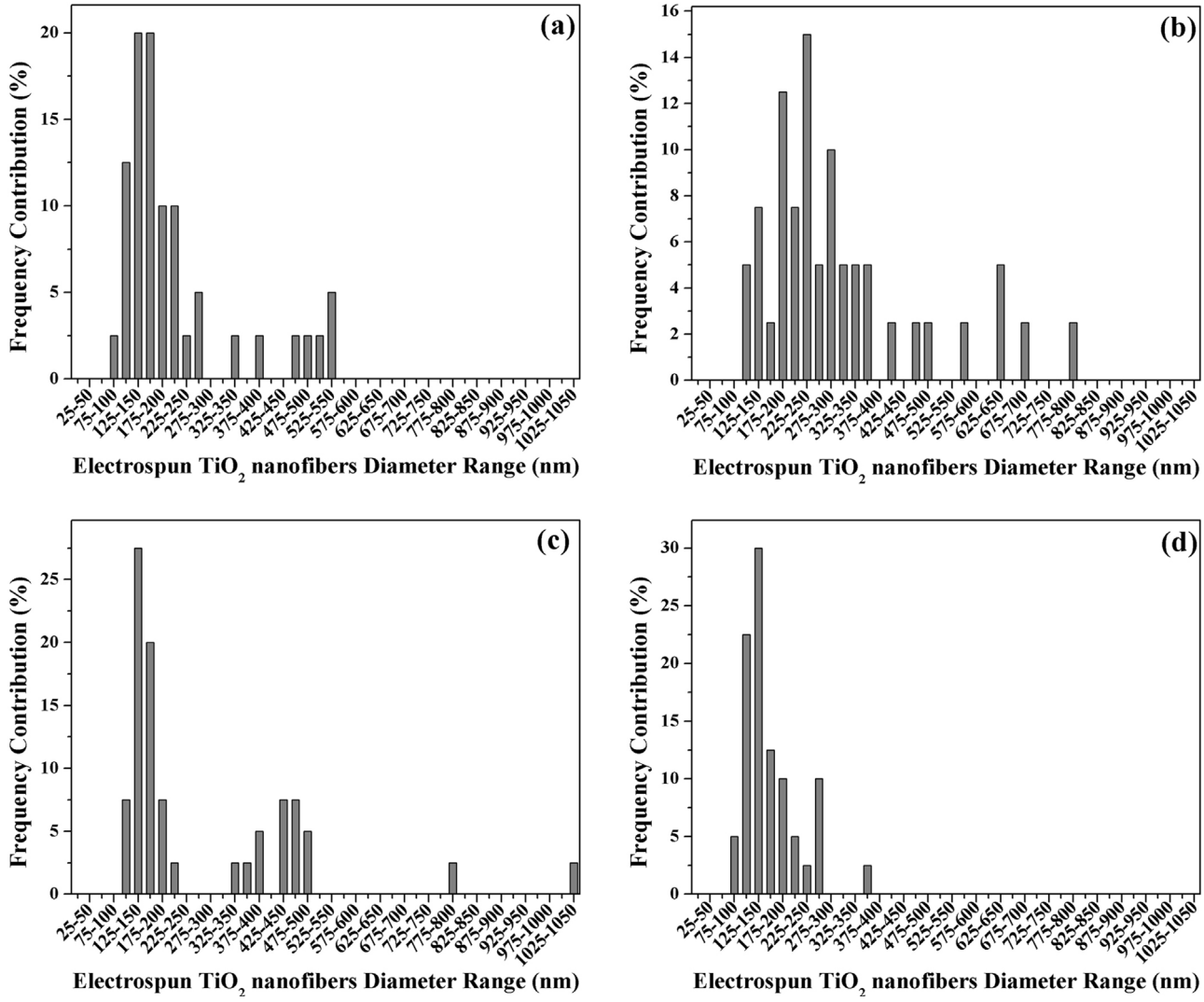

Fig. 4. Frequency contributions to electrospun TiO_2/PVP nanofibers diameter range in DoE study: (a) T1, (b) T2, (c) T3, (d) T4, (e) T5, (f) T6, (g) T7, (h) T8, and (i) T9.

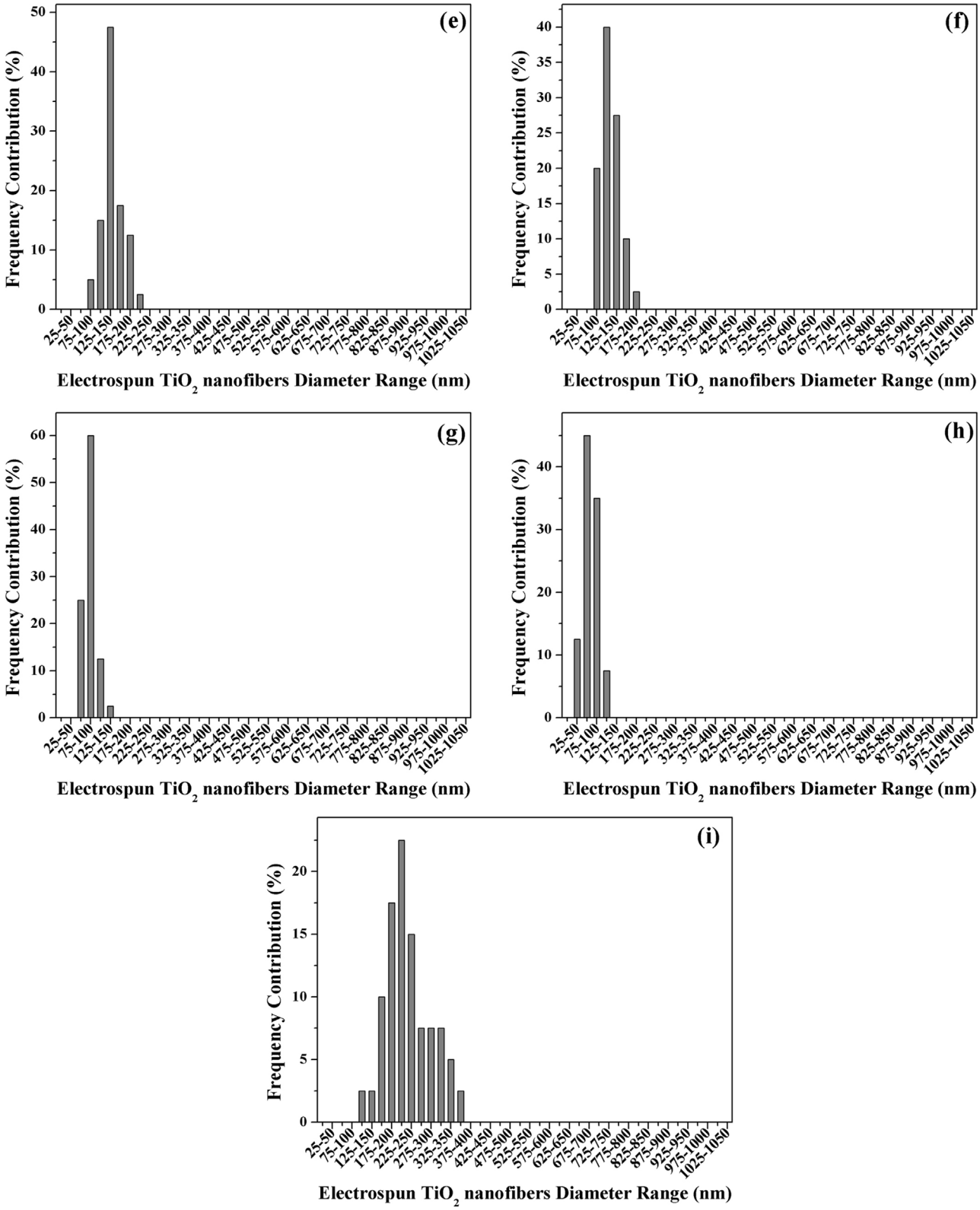

Fig. 4. (*Continued*)

data variance [31]. In the ANOVA, the total variation (S_T), the sum of squares of each factor (S_i) and the percentage contribution (%) were computed, respectively [31].

2.5.1. Total variation (S_T)

The total variation (S_T) is the sum of squares of all trial results, which is expressed in the following form:

$$S_T = \left[\sum_{i=1}^{N} \bar{Y}_i^2\right] - \left[\frac{\left(\sum_{i=1}^{N} \bar{Y}_i\right)^2}{N}\right] \quad (1)$$

where $\bar{Y}_i$ is the mean fiber diameter and N is the number of trials in Taguchi DoE study.

2.5.2. Total variance of each factor (S_i)

$$S_A = \frac{A_{40}^2}{3} + \frac{A_{50}^2}{3} + \frac{A_{60}^2}{3} - C.F \quad (2)$$

$$S_B = \frac{B_{0.5}^2}{3} + \frac{B_1^2}{3} + \frac{B_2^2}{3} - C.F \quad (3)$$

$$S_C = \frac{C_a^2}{3} + \frac{C_b^2}{3} + \frac{C_c^2}{3} - C.F \quad (4)$$

$$S_D = \frac{D_{14}^2}{3} + \frac{D_{18}^2}{3} + \frac{D_{25}^2}{3} - C.F \quad (5)$$

where S_A, S_B, S_C, and S_D are the sum squares for four factors of TiP concentration, flow rate, needle tip-to-collector distance, and applied voltage at three different levels, respectively. $C.F$ is denoted as the correction factor, which is a term similar to the $\left[\left(\sum_{i=1}^{N} \bar{Y}_i\right)^2/N\right]$ in Eq. (1) and it remains constant for all factors. The correction factor ($C.F$) is used for the calculation of all sums of squares [31].

2.5.3. Percentage contribution (%)

The percentage contribution of four factors (P_A, P_B, P_C, or P_D) is the ratio of the total variance of each factor (S_A, S_B, S_C, or S_D) to total variation (S_T) as given by:

$$P_i = \frac{S_i}{S_T} \times 100 \quad (6)$$

where i is the number of factors ($i = 4$ for this study).

2.5.4. Signal to noise ratio (S/N) of electrospun TiO_2 nanofiber diameter

A "smaller the better" characteristic formula [17,28,29,31] has been used to identify the optimum combination of factors to reduce both the fiber diameter and its variation in electrospun TiO_2/PVP nanofibers as indicated below:

$$\mathrm{S/N} = -10 \log\left(\frac{1}{n}\sum_{i=1}^{n} y_i^2\right) \quad (7)$$

where S/N is the signal-to-noise ratio, n is the number of measurements, and y is the diameter of electrospun TiO_2/PVP nanofibers. Mathematically the greater the value of S/N, the smaller the variance for electrospun TiO_2/PVP nanofibers.

3. Characterization

3.1. Scanning electron microscopy (SEM)

Electrospun TiO_2/PVP nanofibers were sputter coated with 3 nm platinum layers to be electrically conductive for reducing the surface charge issue. The surface morphologies of the samples were examined using an EVO 40XVP scanning electron microscope at an accelerating voltage of 15 kV and the magnification of 3000× with a working distance at 8.5 mm. Energy dispersive X-ray spectroscope (EDS) at an acceleration voltage of 10 kV was also used to qualitatively analyze the elemental compositions.

Table 3
Changes in nanofiber diameters of electrospun TiO_2/PVP.

Trial	Combination of factors	Average nanofiber diameter and standard deviation (nm)	S/N
T1	$A_{40}B_{0.5}C_aD_{14}$	218 ± 126	−47.99
T2	$A_{40}B_1C_bD_{18}$	305 ± 165	−50.78
T3	$A_{40}B_2C_cD_{25}$	271 ± 203	−50.56
T4	$A_{50}B_{0.5}C_bD_{25}$	162 ± 59	−44.73
T5	$A_{50}B_1C_cD_{14}$	142 ± 28	−43.21
T6	$A_{50}B_2C_aD_{18}$	118 ± 25	−41.61
T7	$A_{60}B_{0.5}C_cD_{18}$	85 ± 18	−38.81
T8	$A_{60}B_1C_aD_{25}$	70 ± 18	−37.22
T9	$A_{60}B_2C_bD_{14}$	227 ± 57	−47.37

3.2. Imaging analysis

The electrospun nanofiber diameters from the SEM images were measured by *ImageJ*® software (version 1.48e) developed by the National Institutes of Health (NIH), USA. The number of pixels over the scale bar in the SEM image was calibrated by the given length of the scale bar in the corresponding image. Subsequently, the fiber length perpendicular to the fiber axis was measured manually for each fiber. The total number of fiber measurements was 40 in each SEM image and associated average nanofiber diameters along with their standard deviations were calculated accordingly.

4. Results and discussion

4.1. Nanofiber morphology and diameter

SEM micrographs of electrospun nanofiber morphology for the L_9 DoE are illustrated in Fig. 2. The randomly oriented nanofibers had smooth surfaces along with most of large beads as typical defects except that only minor bead defects are noticed in Fig. 2e–g. Fig. 3 shows a typical EDS spectrum of the DoE study with elemental signals for Ti, O, Pt, and C, where Ti and O elements are assigned to TiO_2, as well as C and Pt elements are due to PVP polymer and the platinum coating, respectively [14].

Fig. 4 shows the frequency contribution diagrams for the DoE study in the diameter range of 25–1050 nm. The corresponding average fiber diameters and standard deviations are illustrated in Table 3. T2 in the DoE study yielded the highest average diameter (305 ± 165 nm) with the highest range of variation in diameter (125–1050 nm). The highest viscosity level of the sol–gel solution with 40% TiP concentration and the lowest needle tip-to-collector distance (position b) were the main reasons for the increased nanofiber diameter. However, nanofiber diameter decreased slightly for T1, T3, and T9, where the average diameters and the standard deviations were 218 ± 126 nm, 271 ± 203 nm, and 227 ± 57 nm, respectively. Both T1 and T3 had the same sol–gel concentrations as opposed to T2 with 40 wt% TiP, but with different electrospinning parameters. The needle tip-to-collector distance for T1 (position a) and T3 (position c) was higher than that for the T2 (position b), which was one reason for decreasing fiber diameter. Other reasons to achieve this were to reduce the flow rate or increase the applied voltage. T1 had the lowest level of flow rate (0.5 ml/h), but it also had the lowest level of the applied voltage (14 kV). T3 had the highest level of the applied voltage (25 kV), but also had the highest level of the flow rate (2 ml/h). For T9,

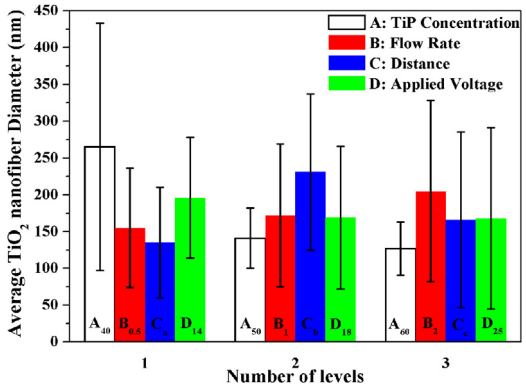

Fig. 5. The effect of TiP concentration, flow rate, needle tip-to-collector distance, and applied voltage on the average nanofiber diameter of electrospun TiO_2/PVP.

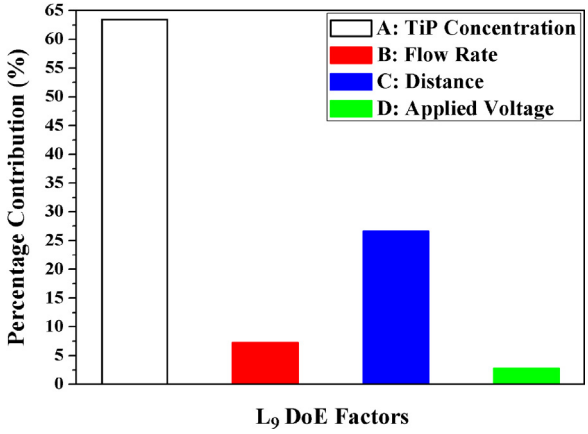

Fig. 6. ANOVA diagram for the determination of significant factors to influence electrospun TiO_2/PVP nanofiber diameters.

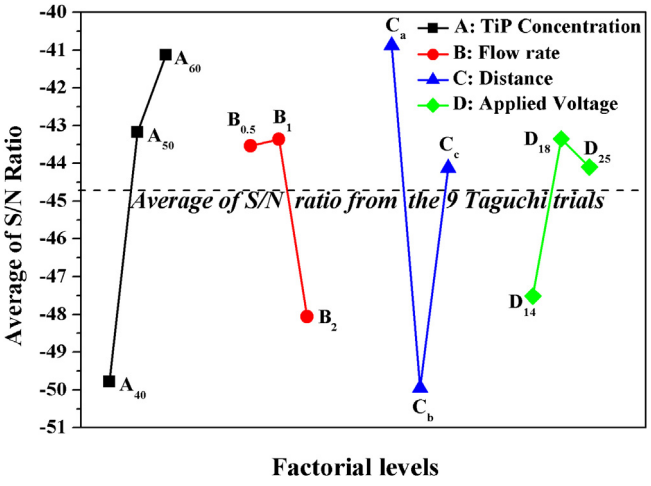

Fig. 7. Average S/N ratio diagram for the determination of the optimum combination of factors for electrospun TiO_2/PVP nanofibers with the smallest fiber diameter size and its minimum variation.

the main reason for the reduction in the diameter size was the TiP concentration of 60 wt%, despite its lowest distance (position *b*), lowest applied voltage (14 kV), and highest flow rate (2 ml/h). The TiP concentration of T4, T5, and T6 was 50 wt%, but with different combinations of electrospinning factors. Most of the diameter variation was from 75 to 275 nm, and the average diameters were under 200 nm. For both T7 and T8, the highest level of TiP concentration at 60 wt% was used. The average fiber diameters and the standard deviations were 85 ± 18 nm for T7, and 70 ± 18 for T8 due to different electrospinning conditions. Both T7 and T8 had a minimum variance of fiber diameter, where about 80% frequency contribution was detected in the fiber diameter range of 50–100 nm. Fig. 5 shows the effect of TiP concentration, flow rate, needle tip-to-collector distance, and applied voltage on the average nanofiber diameter of electrospun TiO_2/PVP. It was found that the fiber diameters decreased with increasing the TiP concentration (a decrease in viscosity due to the low concentration of PVP polymer in the TiP/PVP solution), needle tip-to-collector distance (position *a*) and applied voltage setting while decreasing the flow rate, which is in good agreement with previous literature [11,17,20]. The nanofiber diameters decreased relatively sharply from 265 nm with the 40 wt% TiP to 127 nm with 60 wt% TiP. This finding suggests that the TiP concentration is the most significant factor for achieving the small nanofiber diameter of electrospun TiO_2/PVP with the minimum variance (a further detail is included in the Taguchi analysis).

4.2. Analysis of variance (ANOVA)

The relative percentage contributions of electrospinning factors were determined using Eqs. (1)–(6). The ANOVA diagram depicted in Fig. 6 demonstrates that the effect of processing parameters on nanofiber diameters of electrospun TiO_2/PVP by the percentage contributions for selected L_9 DoE factors. The TiP concentration (factor A) was a significant variable to control the nanofiber diameter with a percentage contribution of 63.45%. This provides the further evidence that increasing the TiP concentration decreases the diameter size. The second and third most prevalent factors in minimizing nanofiber diameters were the needle tip-to-collector distance (factor C) and the flow rate (factor B) with the percentage of contributions of 26.59% and 7.23% accordingly. The applied voltage (factor D) appeared to be insignificant at 2.72% only. It is implied that the applied voltage has a trivial impact on the nanofiber diameter, which can be maintained at the workable experimental range.

4.3. Optimum combination of factors

The S/N ratios for electrospun TiO_2/PVP nanofibers were calculated using the "smaller the better" Eq. (7) for the nine Taguchi DoE study (Table 3). Since the purpose of this research work is to determine the smallest nanofiber with the minimum variance, the highest value of S/N ratio yields the optimum condition from the Taguchi DoE work [17,28,31]. As illustrated in Table 3, T8 ($A_{60}B_1C_aD_{25}$) was determined to be the best candidate for inclusion in the optimal combination, which has the maximum S/N value of −37.22 with the average nanofiber diameter and standard deviation at 70 ± 18 nm. However, T7 ($A_{60}B_{0.5}C_cD_{18}$) with the S/N value of −38.81 and the average fiber diameter and standard deviation at 85 ± 18 nm is another strong candidate. The average fiber diameter for T8 is slightly smaller than that for T7, but the fiber variance for T7 is less than that for T8, and the standard deviation is ±18 nm in both cases. In Fig. 4, 60% frequency contribution of fibers in the nanofiber diameter range from 75 to 100 nm for T7; whereas for T8, it is 45% in the diameter range of 50 to 75 nm, and 35% between 75 and 100 nm.

Therefore, the average S/N ratio was calculated to determine the best level factor for the optimum contribution to minimize the diameter and variation of electrospun TiO_2/PVP nanofibers as shown in Fig. 7. It suggests that 60 wt% TiP concentration, a flow rate of 1 ml/h, needle tip-to-collector distance (position *a*), and applied voltage of 18 kV ($A_{60}B_1C_aD_{18}$) is the optimum combination of factors to obtain small electrospun TiO_2/PVP nanofiber with the minimum variation. It is further proven that the TiP concentration and the needle tip-to-collector distance are the two most

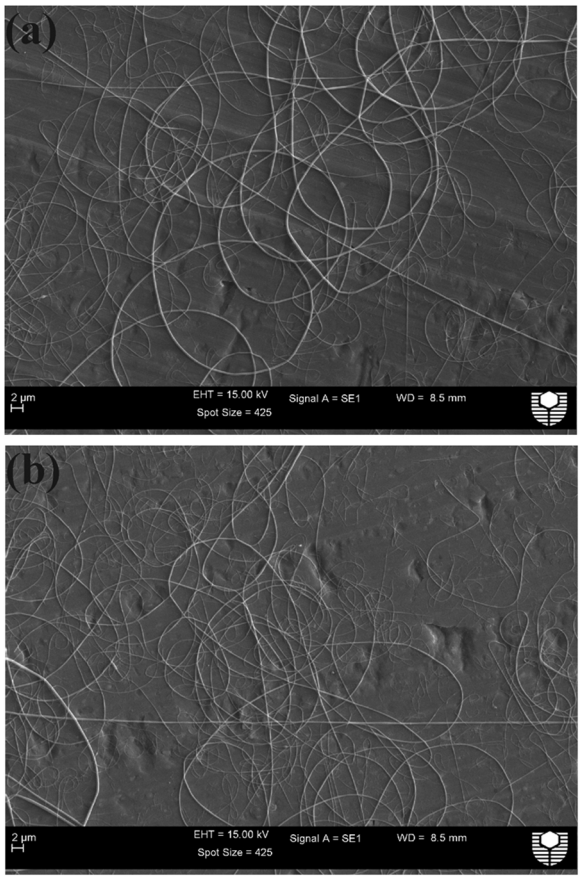

Fig. 8. SEM micrographs of the confirmation experiment for the optimum combination of factors ($A_{60}B_1C_aD_{18}$) using two different needle sizes: (a) 0.514 mm and (b) 0.819 mm. All scale bars represent 2 μm.

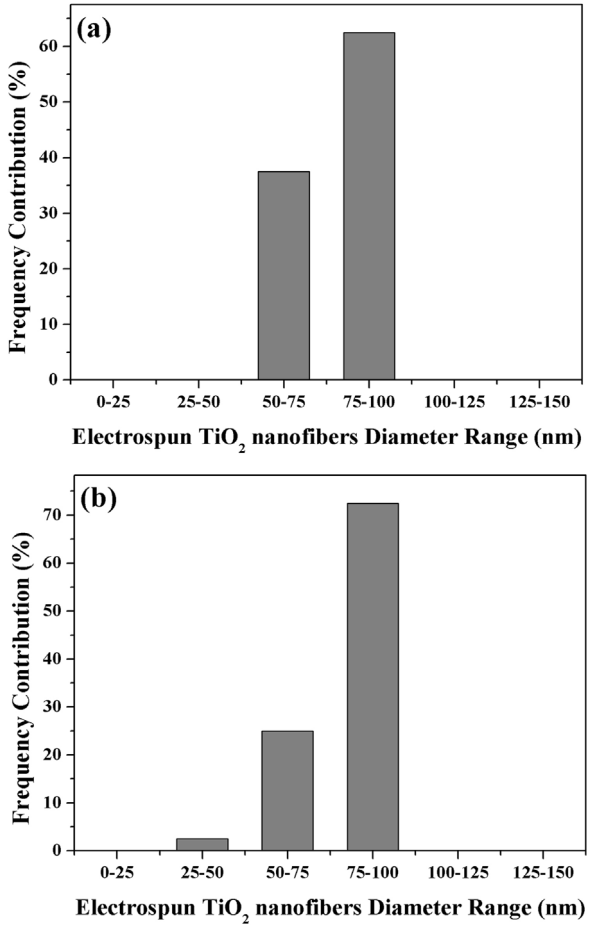

Fig. 9. Frequency contributions to electrospun TiO_2/PVP nanofibers diameter range for confirmation experiments using needle sizes of (a) 0.514 mm and (b) 0.819 mm.

significant factors; whereas the flow rate and the applied voltage appear to be relatively insignificant.

4.4. Confirmation experiment to optimum conditions

The confirmation experiment for the optimum combination of factors was subsequently carried out as a necessary and important post-step in the Taguchi DoE method [31]. The optimum combination ($A_{60}B_1C_aD_{18}$) was tested with the same needle size of 0.514 mm and a new needle size of 0.819 mm to study the effect on the nanofiber diameter of electrospun TiO_2/PVP. Fig. 8 shows the typical SEM images of confirmation experiments with both needle sizes. The randomly oriented nanofibers had smooth surfaces without beads defects in both images. The mean diameter and range are 79 ± 11 nm and 84 ± 13 nm for the confirmation experiments of the needle size of 0.514 mm, and needle size of 0.819 mm, respectively. It is clear that the needle size is a non-significant factor in the nanofiber diameter of electrospun TiO_2/PVP. The diameters of these nanofibers for both needles sizes are compared closely with the best Taguchi candidate values obtained in T7 (85 ± 18), and T8 (70 ± 18). The T8 gives the smallest nanofiber diameter, but the optimum combination ($A_{60}B_1C_aD_{18}$) gives comparatively small electrospun TiO_2/PVP nanofiber diameter with the smallest standard deviation. In Fig. 9, most the frequency contribution diagrams for both confirmation experiments are presented in the fiber diameter range of 50–100 nm with smallest standard deviations, as compared to the orthogonal array with nine trials (L_9).

5. Conclusions

An L_9 orthogonal array along with S/N ratios and ANOVA in Taguchi DoE method was used to investigate TiP concentration, flow rate, needle tip-to-collector distance, and applied voltage at three different levels on the nanofiber diameter of electrospun TiO_2/PVP. The small nanofiber diameter with the minimum variance has been found to be controlled mainly by two significant factors, namely TiP concentration, and needle tip-to-collector distance. The optimum combination of factors with the highest level of the TiP concentration, and the highest relative needle tip-to-collector distance (position *a*) was found along with a flow rate of 1 ml/h and an applied voltage setting of 18 kV ($A_{60}B_1C_aD_{18}$). The effects of the needle size on the nanofiber diameter and its variation of electrospun TiO_2/PVP were also investigated based on this optimal combination. It was determined that the needle size is a non-significant factor in the nanofiber diameter of electrospun TiO_2/PVP.

Acknowledgments

The authors wish to acknowledge Mrs. E. Miller for the technical assistance with SEM analysis. Moreover, H. Albetran is grateful to the College of Education - Dammam, University of Dammam, Saudi Arabia for the financial support in the form of a PhD Scholarship.

References

[1] P. Panda and S. Ramakrishna, J. Mater. Sci., 42, 2189–2193 (2007).

[2] J.Y. Park and S.S. Kim, Met. Mater. Int., 15, 95–99 (2009).
[3] C. Wang, Y. Tong, Z. Sun, Y. Xin, E. Yan and Z. Huang, Mater. Lett., 61, 5125–5128 (2007).
[4] W. Sigmund, J. Yuh, H. Park, V. Maneeratana, G. Pyrgiotakis, A. Daga, J. Taylor and J.C. Nino, J. Am. Ceram. Soc., 89, 395–407 (2006).
[5] Y. Dong, T. Mosaval, H.J. Haroosh, R. Umer, H. Takagi and K.T. Lau, J. Polym. Sci. Part B: Polym. Phys., 52, 618–623 (2014).
[6] H. Wu, W. Pan, D. Lin and H. Li, J. Adv. Ceram., 1, 2–23 (2012).
[7] T. Jamnongkan, R. Shirota, S.K. Sukumaran, M. Sugimoto and K. Koyama, SPE Plast. Res. Online, (2013), http://dx.doi.org/10.2417/spepro.005181
[8] J.Y. Park, J.J. Yun, C.H. Hwang and I.H. Lee, Mater. Lett., 64, 2692–2695 (2010).
[9] M. Samadi, H.A. Shivaee, M. Zanetti and A. Moshfegh, J. Mol. Catal. A: Chem., 359, 42–48 (2012).
[10] D.A. Hanaor and C.C. Sorrell, J. Mater. Sci., 46, 855–874 (2011).
[11] H. Li, W. Zhang, B. Li and W. Pan, J. Am. Ceram. Soc., 93, 2503–2506 (2010).
[12] Q. Li, D.J.G. Satur, H. Kim and H.G. Kim, Mater. Lett., 76, 169–172 (2012).
[13] C. Wessel, R. Ostermann, R. Dersch and B.M. Smarsly, J. Phys. Chem. C, 115, 362–372 (2011).
[14] H. Albetran, H. Haroosh, Y. Dong, V. Prida, B. O'Connor and I. Low, Appl. Phys. A, 116, 161–169 (2014).
[15] Z.M. Huang, Y.Z. Zhang, M. Kotaki and S. Ramakrishna, Compos. Sci. Technol., 63, 2223–2253 (2003).
[16] S.V. Fridrikh, J.H. Yu, M.P. Brenner and G.C. Rutledge, Phys. Rev. Lett., 90, 144502–144506 (2003).
[17] S. Patra, A. Easteal and D. Bhattacharyya, J. Mater. Sci., 44, 647–654 (2009).
[18] R. Inai, M. Kotaki and S. Ramakrishna, Nanotechnology, 16, 208–213 (2005).
[19] D. Li and Y. Xia, Nano Lett., 3, 555–560 (2003).
[20] A. Kumar, R. Jose, K. Fujihara, J. Wang and S. Ramakrishna, Chem. Mater., 19, 6536–6542 (2007).
[21] C.M. Wu, H.G. Chiou, S.L. Lin and J.M. Lin, J. Appl. Polym. Sci., 126, 89–97 (2012).
[22] B. Ksapabutr, T. Chalermkiti and M. Panapoy, Chiang Mai Univ. J., 4, 115–119 (2005).
[23] O. Hardick, B. Stevens and D.G. Bracewell, J. Mater. Sci., 46, 3890–3898 (2011).
[24] W.K. Son, D. Cho and W.H. Park, Nanotechnology, 17, 439–443 (2006).
[25] J.A. Park, J. Moon, S.J. Lee, S.H. Kim, T. Zyung and H.Y. Chu, Thin Solid Films, 518, 6642–6645 (2010).
[26] W. Nuansing, S. Ninmuang, W. Jarernboon, S. Maensiri and S. Seraphin, Mater. Sci. Eng. B, 131, 147–155 (2006).
[27] S. Chuangchote, J. Jitputti, T. Sagawa and S. Yoshikawa, ACS Appl. Mater. Interfaces, 1, 1140–1143 (2009).
[28] Y. Dong, T. Bickford, H.J. Haroosh, K.T. Lau and H. Takagi, Appl. Phys. A, 112, 747–757 (2013).
[29] J. Ghani, I. Choudhury and H. Hassan, J. Mater. Process. Technol., 145, 84–92 (2004).
[30] Y. Dong and D. Bhattacharyya, Composites Part A: Appl. Sci. Manuf., 39, 1177–1191 (2008).
[31] R. Ranjit, A Primer on the Taguchi Method, van Nostrand Reinhold, New York (1990).